Supplemental Material

METHODS

Animal Model of Atherothrombosis

New Zealand white rabbits (n=31, weight 3-4kg, Charles River Laboratories) at 3-4 months of age consumed a 1% high cholesterol diet (HCD, Research Diets, Inc., New Brunswick, NJ) for 2 weeks prior to aortic balloon injury of the abdominal aorta followed by another six weeks of 1% HCD and four weeks of normal chow diet (Supplemental Figure 1).[1, 2] Balloon injury using a 3F Fogarty catheter inflated to tension was performed over a 6cm segment of the abdominal aorta distal to the renal arteries using fluoroscopic guidance. Balloon injury and imaging were performed under general anesthesia using ketamine 45mg/kg and xylazine 5.5mg/kg for induction and maintenance with inhaled 2% isoflurane.

Synthesis of CLIO-CyAm7, a NIR fluorescent ultrasmall superparamagnetic iron oxide nanoparticle. Crosslinked iron oxide (CLIO) nanoparticles were obtained from the Center for Systems Biology Chemistry Core at Massachusetts General Hospital (Supplemental Figure 2). Into 400 µL of dimethylsulfoxide, 2 mg of the NIR fluorophore CyAm7 (λ_{max} absorption = 744 nm, λ_{max} emission = 769 nm) was dissolved and added to 40 mg of CLIO (9.98 mg Fe/mL in PBS). The reaction was allowed to proceed for 16 hours, at which time it was filtered through Sephadex G25 to yield the conjugate (CLIO-CyAm7, 5.0 mg Fe/mL, 1.4×10^{-4} M CyAm7).

CLIO-CyAm7 deposition in atherosclerosis and atherothrombosis protocol. Ten weeks after balloon injury, CLIO-CyAm7 (2.5 mg Fe/kg, n=21) or saline (n=3) was

injected intravenously. At twenty-four hours, 9 rabbits were sacrificed for histological assessment and 15 rabbits underwent pharmacologic triggering to induce plaque thrombosis. For pharmacologic triggering, Russell's viper venom (0.15 mg/kg IP, Sigma Chemical Co) followed 30 minutes later by histamine (0.02 mg/kg IV, Sigma Chemical Co) were injected twice at a 24-hour interval.[1, 2] Rabbits were imaged pre-trigger (angiography, 2D NIRF imaging, intravascular ultrasound (IVUS)) and 48-hours post-trigger (angiography, IVUS). Rabbits were then sacrificed and perfused with saline.

In vivo intra-arterial NIRF molecular Imaging and IVUS structural imaging

NIRF imaging of atheroma cellularity. Custom-built standalone 2D NIRF catheter-based system utilizes continuous wave NIR fiber-coupled laser with excitation light of 750nm.[3] The NIRF fiber was placed percutaneously through the carotid artery into the rabbit aorta under fluoroscopic guidance. The fiber was mechanically rotated and retracted to produce a 2D image of the vessel wall (MATLAB R2011a MathWorks). Four 90-100cm pullbacks from the iliac bifurcation to the renal arteries were performed, with two different placements of the guidewire. NIRF imaging was performed through blood, without flushing, as light penetrates efficiently in the NIR window.[4]

2D NIRF signal analysis. The raw NIRF signal was filtered using a low pass filter and background subtraction. The signal was then averaged over 3 mm segments along the length of the aorta (MATLAB).[3] The maximum signal in a 3 mm segment along multiple pullbacks was calculated (Supplemental Figure 3). Signal from vessels of diameter greater than 5 mm on IVUS due to aneurysm formation were excluded from NIRF analysis given the high degree of NIR light attenuation in larger diameter vessels. NIRF images were quantified using target-to-background ratio (TBR), defined as the signal from an area of plaque divided by the signal from a normal, uninjured segment of the

aorta. The length of the aorta was divided into six 1.5 cm segments and correlated with *ex vivo* imaging and histology for analysis. The maximal TBR from all pullbacks in each segment was calculated (MATLAB). Segments were characterized as either plaque or normal vessel based on neointimal thickening on pre-trigger IVUS imaging or microscopy.

IVUS Structural assessment of atherosclerosis and atherothrombosis. IVUS imaging (Galaxy IVUS System, Boston scientific, Natick, MA) was performed pre- and post-pharmacologic thrombus triggering. One rabbit did not undergo IVUS post-trigger imaging due to technical difficulties. IVUS was co-registered with NIRF imaging using fluoroscopy of the radiopaque marker at the end of the IVUS catheter before and after imaging. Pre- and post-IVUS images were co-registered to each other using side branches as fiducials. Thrombi were identified on cross-sectional post-trigger IVUS imaging as new luminal defects. IVUS images were further reconstructed into 6 long axis images for additional visualization of luminal thrombi and comparison to NIRF imaging (MATLAB). The vessel diameter was calculated as the average diameter along two perpendicular planes on cross sectional images.

Endothelial permeability studies. The relationship between CLIO-CyAm7 nanoparticle deposition and impaired endothelial permeability was assessed by Evans Blue dye leakage[5] in a separate cohort of rabbits (n=7) who were intravenously injected with Evans Blue (6 mL 0.5%, Sigma Chemical Co) 30 minutes prior to sacrifice.[5] A higher dose of CLIO-CyAm7 (5.0 mg/kg IV 24 hours prior to sacrifice) was used to overcome fluorescence overlap with Evans Blue.

Fluorescence Reflectance Imaging (FRI)

After sacrifice, FRI was performed to image CLIO-CyAm7 fluorescence signal along the length of the aorta (Kodak Carestream 4000 MMPro). For FRI, the resected aorta was elongated to the *in vivo* length determined by angiography and imaged in NIR (excitation 716 to 756 nm, emission 780 to 820 nm, 16 seconds) and white light. The target signal for analysis was defined as a 3 cm area of atheroma manually traced in the area of balloon injury (ImageJ, NIH, Bethesda MD). The background noise was measured in an adjacent image region measuring the same area as the target region. The uninjured renal artery was utilized as a control vessel. For FRI imaging, the renal artery was selected as the preferred control segment as it was not instrumented at all during the initial balloon injury with sheath, guidewire or Fogarty balloon delivery. As the renal artery was too small for in vivo imaging, the larger uninjured aorta was used as the control vessel for in vivo imaging and the corresponding microscopy. The signal-to-noise ratio (SNR) was calculated for all non-triggered rabbits (n=6) as the target atheroma signal divided by the standard deviation of background noise.[3] The target-to-background ratio (TBR) was defined as the target atheroma signal divided by the signal from the control uninjured renal artery.

Histological Assessment of CLIO-CyAm7 and Atherothrombosis

Histology, immunofluorescence (IF), and immunohistochemistry (IHC). Resected aortas were elongated to *in vivo* length as determined by presacrifice angiography, systematically divided into 1.5 cm segments and marked with tissue marking ink for co-registration. Then, 0.5 cm segments were embedded in OCT (Sakura, Finetek, Torrance, CA), flash frozen, and cryosectioned (6μm). Sections were stained using Carstairs' stain to assess general morphology and collagen structure (blue) and to identify fibrin rich thrombi (red). Adjacent sections were stained by IF and IHC using the antibodies RAM11 for macrophages, CD31 for endothelial cells, and α-smooth muscle actin (aSMA)

for SMCs.

Immunohistochemistry (IHC) and immunofluorescence (IF) antibodies used for staining: RAM11 for macrophages (Dako, IF 1:200, IHC 1:500), CD31 for endothelial cells (Abcam, IF 1:200, IHC 1:100), and α-smooth muscle actin (aSMA) for SMCs (Abcam, IF 1:200, IHC 1:100). All stains were performed on an uninjured renal artery section for controls. For IF, secondary goat anti-mouse Texas Red antibody (1:200 dilution, Abcam) was used. RAM11 IHC was incubated with secondary anti-mouse Alkaline Phosphatase-conjugated antibody, stained using Vulcan fast red chromagen (Biocare medical). CD31 and aSMA IHC used biotin-streptavidin conjugation for visualization. All IHC sections were counterstained with hematoxylin.

Fluorescence microscopy of CLIO-CyAm7 deposition in atheroma. CLIO-CyAm7 was visualized on histological sections using customized NIR filters (Eclipse 90i, Nikon Instruments, ex/em: 710/810 nm, 500 ms exposure). The fluorescence distribution of Evans blue and secondary antibodies (RAM11, CD31, and aSMA) were imaged using a Texas Red filter (ex/em 590/620 nm, 100ms exposure). Autofluorescence (ex/em 480/535 nm; 500 ms exposure) was measured during all FM studies. Epifluorescence microscopy images were acquired at 40x magnification.

CLIO-CyAm7 microscopic accumulation was analyzed on FM at 0.5 cm intervals along the aorta (n=183 sections). Of the 183 microscopy sections analyzed, each section was classified as plaque (n=144) or normal (n=39), based on the presence of intimal thickening on autofluorescence-based microscopy. Each atheroma section was further defined as thrombosed (n=38) or non-thrombosed (n=106) based on Carstairs' stain evidence of adherent fibrin-rich thrombi. For quantitative fluorescence analysis, an FM

image of the entire plaque was obtained from unstained, non-coverslipped sections at 10x magnification. A signal intensity threshold was determined visually to limit background NIR fluorescence and applied equally to all images. After thresholding, a region of interest (ROI) to analyze superficial intimal CLIO-CyAm7 signal was defined as all tissue within 100 μm of the luminal edge. One section from each 0.5 cm segment of aorta was analyzed using this method, and the maximum percent positive area of three sections across a 1.5 cm segment (previously demarcated with tissue marking ink to correspond with *in vivo* imaging) was used for further analysis of each segment (normal vessel n=25; atheroma without thrombus, n=30; atheroma with adherent thrombus, n=21). All analyses were performed using ImageJ (NIH, Bethesda, MD).

Statistical Analysis

Statistical analyses were completed using GraphPad Prism (v5.0 GraphPadSoftware, San Diego, CA). Appropriate threshold for specificity and sensitivity calculations were determined using an ROC curve for optimization. For all 2D NIRF TBR and microscopy analyses between two groups, the nonparametric Mann-Whitney U test was used. Data is presented as mean ± standard deviation.

References

1. Phinikaridou A, Hallock KJ, Qiao Y, Hamilton JA. A robust rabbit model of human atherosclerosis and atherothrombosis. *Journal of lipid research*. 2009;50:787-797
2. Phinikaridou A, Ruberg FL, Hallock KJ, Qiao Y, Hua N, Viereck J, Hamilton JA. In vivo detection of vulnerable atherosclerotic plaque by MRI in a rabbit model. *Circulation. Cardiovascular imaging*. 2010;3:323-332
3. Jaffer FA, Calfon MA, Rosenthal A, Mallas G, Razansky RN, Mauskapf A, Weissleder R, Libby P, Ntziachristos V. Two-dimensional intravascular near-infrared fluorescence molecular imaging of inflammation in atherosclerosis and stent-induced vascular injury. *Journal of the American College of Cardiology*. 2011;57:2516-2526
4. Osborn EA, Jaffer FA. The year in molecular imaging. *JACC. Cardiovascular imaging*. 2010;3:1181-1195

5. Phinikaridou A, Andia ME, Protti A, Indermuehle A, Shah A, Smith A, Warley A, Botnar RM. Noninvasive magnetic resonance imaging evaluation of endothelial permeability in murine atherosclerosis using an albumin-binding contrast agent. *Circulation*. 2012;126:707-719

Supplemental Figure Legends

Supplemental Figure 1. Rabbit atherothrombosis protocol. Schematic of timeline for rabbit triggered thrombosis. Alternating 1% high cholesterol diet (HCD) with normal chow diet starting two weeks prior to aortic balloon injury. After completion of the twelve-week diet protocol, rabbits underwent pharmacologic triggering and in vivo survival imaging with near infrared fluorescence (NIRF) and intravascular ultrasound (IVUS) imaging. Pharmacologic triggering, with Russell's viper venom followed by histamine injections, occurred twice, twenty-four hours apart. At forty-eight hours after initial triggering, in vivo IVUS imaging was performed followed by sacrifice and ex vivo studies.

Supplemental Figure 2. Schematic of CLIO-CyAm7 nanoparticle. Representation of the synthesized CLIO-CyAm7 particle with an ultrasmall paramagnetic iron oxide (USPIO) nanoparticle core conjugated to an NIR fluorophore CyAm7.

Supplemental Figure 3. Example analysis of in vivo NIRF imaging in a single rabbit. Due to distance-dependent attenuation of NIRF signal, imaging pullbacks were repeated four times to account for the variation in placement of the catheter in relation to the arterial wall. (A) Four pullbacks were aligned using the radiopaque catheter tip under fluoroscopy and the maximum TBR was calculated along 360 degrees for 3 mm segments. Each pullback was graphed in a different color. (B) The maximum TBR was identified from all pullbacks along the length of the aorta and used for further analysis.

Supplemental Figure 4. Receiver operator curve (ROC) for fluorescence microscopy. (A,B) Histogram of values for fluorescence microscopy percent positive CLIO CyAm7 pixels represented linearly and on a logarithmic scale. (C) ROC curve of

sensitivity and specificity for determination of optimal threshold of percent positive area. The optimal threshold was determined to be 0.85% positive pixels, which represents a likelihood ratio of 2.16.

Supplemental Figure 1:

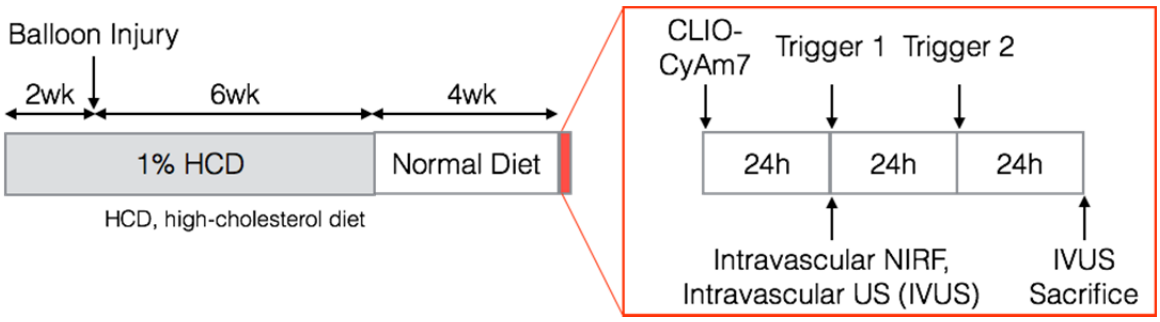

Supplemental Figure 2:

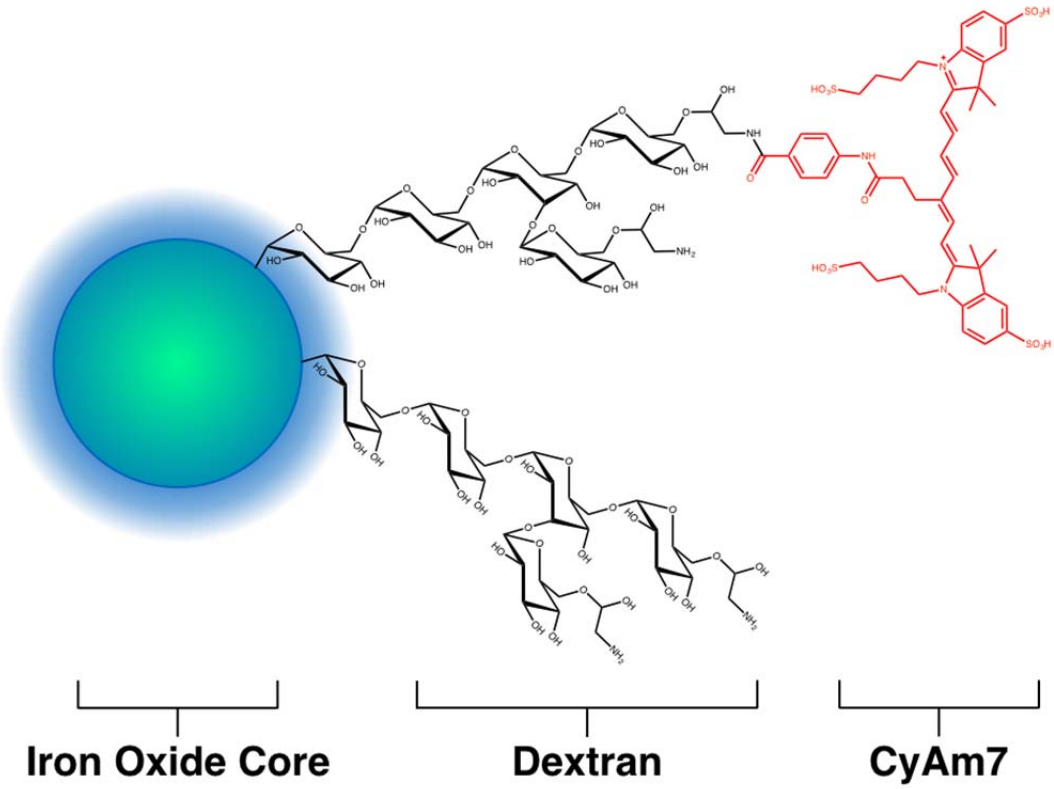

Supplemental Figure 3:

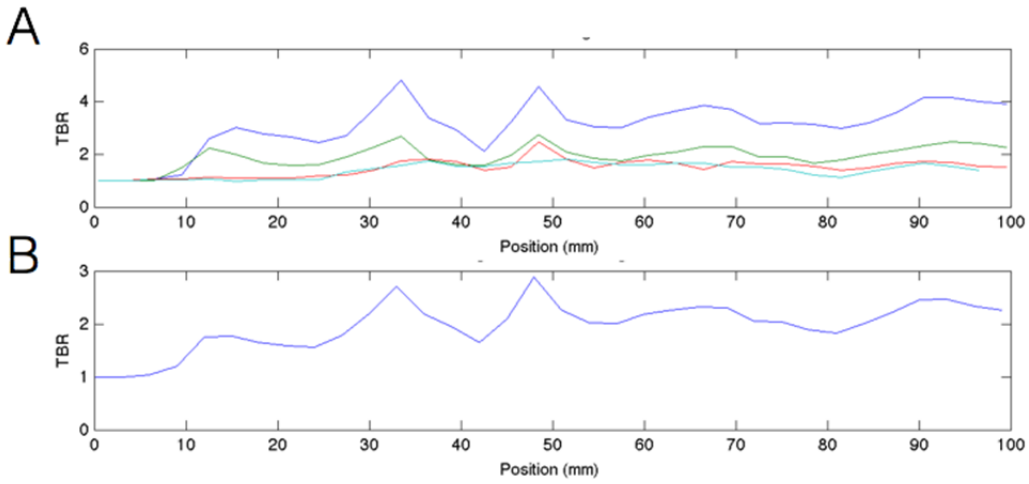

Supplemental Figure 4